ISSN 1674-1056
http://cpb.iphy.ac.cn
http://iopscience.iop.org/cpb
中国物理 B
Chinese Physics
中国物理 Chinese Physics B

Low-temperature synthesis of apatite-type $La_{9.33}Ge_6O_{26}$ as electrolytes with high conductivity

Guang-Chao Yin(尹广超), Guo-Dong Zhao(赵国栋), Hong Yin(殷红), Fu-Chao Jia(贾福超), Qiang Jing(景强), Sheng-Gui Fu(付圣贵), Mei-Ling Sun(孙美玲), Wei Gao(高伟)
Citation: Chin. Phys. B . 2018, 27(4): 048201. **doi:** 10.1088/1674-1056/27/4/048201

Journal homepage: http://cpb.iphy.ac.cn; http://iopscience.iop.org/cpb

What follows is a list of articles you may be interested in

Enhanced ionic conductivity in LAGP/LATP composite electrolyte

Shi-Gang Ling(凌仕刚), Jia-Yue Peng(彭佳悦), Qi Yang(杨琪), Ji-Liang Qiu(邱纪亮), Jia-Ze Lu(卢嘉泽), Hong Li(李泓)
Chin. Phys. B . 2018, 27(3): 038201. **doi:** 10.1088/1674-1056/27/3/038201

Molecular dynamics simulation of the response of bi-disperse polyelectrolyte brushes to external electric fields

Fen Zhang(张芬), Huan-Da Ding(丁欢达), Chao Duan(段超), Shuang-Liang Zhao(赵双良), Chao-Hui Tong(童朝晖)
Chin. Phys. B . 2017, 26(8): 088204. **doi:** 10.1088/1674-1056/26/8/088204

A low cost composite quasi-solid electrolyte of LATP, TEGDME, and LiTFSI for rechargeable lithium batteries

Jie Huang(黄杰), Jia-Yue Peng(彭佳悦), Shi-Gang Ling(凌仕刚), Qi Yang(杨琪), Ji-Liang Qiu(邱纪亮), Jia-Ze Lu(卢嘉泽), Jie-Yun Zheng(郑杰允), Hong Li(李泓), Li-Quan Chen(陈立泉)
Chin. Phys. B . 2017, 26(6): 068201. **doi:** 10.1088/1674-1056/26/6/068201

Particles inside electrolytes with ion-specific interactions, their effective charge distributions and effective interactions

Mingnan Ding(丁茗楠), Yihao Liang(梁逸浩), Xiangjun Xing(邢向军)
Chin. Phys. B . 2016, 25(10): 108201. **doi:** 10.1088/1674-1056/25/10/108201

Concentrated dual-salt electrolytes for improving the cycling stability of lithium metal anodes

Pin Liu(刘品), Qiang Ma(马强), Zheng Fang(方铮), Jie Ma(马洁), Yong-Sheng Hu(胡勇胜), Zhi-Bin Zhou(周志彬), Hong Li(李泓), Xue-Jie Huang(黄学杰), Li-Quan Chen(陈立泉)
Chin. Phys. B . 2016, 25(7): 078203. **doi:** 10.1088/1674-1056/25/7/078203

Low-temperature synthesis of apatite-type $La_{9.33}Ge_6O_{26}$ as electrolytes with high conductivity*

Guang-Chao Yin(尹广超)[1], Guo-Dong Zhao(赵国栋)[1], Hong Yin(殷红)[2], Fu-Chao Jia(贾福超)[1], Qiang Jing(景强)[1], Sheng-Gui Fu(付圣贵)[1], Mei-Ling Sun(孙美玲)[1,†], and Wei Gao(高伟)[2,‡]

[1] *Laboratory of Functional Molecular Materials, School of Physics and Optoelectronic Engineering, Shandong University of Technology, Zibo* 255000, *China*

[2] *State Key Laboratory of Superhard Materials, Jilin University, Changchun* 130012, *China*

(Received 28 November 2017; revised manuscript received 8 January 2018; published online 10 March 2018)

In the present study, high-quality apatite-type $La_{9.33}Ge_6O_{26}$ powders are successfully synthesized by a facile molten-salt synthesis method (MSSM) at low temperatures, using LiCl, LiCl/NaCl mixture (mass ratio 1:1) as molten salt, respectively. Experimental results indicate that the optimal mass ratio between reactant and molten salt is 1:2, and LiCl/NaCl mixed molten-salt is more beneficial for forming high-quality $La_{9.33}Ge_6O_{26}$ powders than LiCl individual molten-salt. Comparing with the conventional solid-state reaction method (SSRM), the synthesis temperature of apatite-type $La_{9.33}Ge_6O_{26}$ powders using the MSSM decreases more than 350 °C, which can effectively avoid Ge loss in the preparation process of precursor powders. Furthermore, the powders obtained by the MSSM are homogeneous, non-agglomerated and well crystallized, which are very favorable for gaining dense pellets in the premise of avoiding Ge loss. On the basis of high-quality precursor powders, the dense and pure ceramic pellets of $La_{9.33}Ge_6O_{26}$ are gained at a low temperature of 1100 °C for 2 h, which exhibit higher conductivities ($\sigma_{850\,^\circ C(LiCl)} = 2.3 \times 10^{-2}$ S·cm^{-1}, $\sigma_{850\,^\circ C(LiCl/NaCl)} = 4.9 \times 10^{-2}$ S·cm^{-1}) and lower activation energies ($E_{a(LiCl)} = 1.02$ eV, $E_{a(LiCl/NaCl)} = 0.99$ eV) than that synthesized by the SSRM.

Keywords: solid oxide fuel cells, electrolyte, ionic conduction

PACS: 82.47.Ed, 82.45.Gj, 66.30.Dn **DOI:** 10.1088/1674-1056/27/4/048201

1. Introduction

Apatite-type lanthanum silicates (ATLS) and apatite-type lanthanum germanates (ATLG), as novel electrolytes for the intermediate temperature solid oxide fuel cells (IT-SOFCs),[1–15] have been attracting widespread attention of the scientific community due to their clean energy conversions, superior ionic conductivities, excellent long-term stabilities and low processing cost. In contrast to the fact that traditional fluorite and perovskite-type oxide ion conductors have a vacancy conduction mechanism,[16–18] apatite-type materials have an especial interstitial oxide ion conduction mechanism,[19,20] which could be responsible for their high oxide-ion conductivities. It has been found that among the apatite-type conductors, ATLG has a higher conductivity than that of ATLS at similar temperatures. However, ATLS have been investigated more extensively than ATLG due to several problems related to Ge loss at high temperature.[21–24]

It is well known that the conductivity of solid electrolytes highly depends on the levels of purity and densification. In general, dense apatite-type ceramics prepared by conventional SSRM require the repeated long-time and high-temperature (1300 °C–1700 °C) sintering. However, high sintering temperature > 1120 °C (melting point of GeO_2) will induce the Ge volatilization loss, further bringing the secondary phase La_2GeO_5 into the samples, finally resulting in the reduction of conductivity.[21–24] Therefore, in order to exhibit their best electrical properties using SSRM, dense ATLG ceramics with high purity are very difficult to obtain. In order to overcome this drawback, some synthesis methods were developed to optimize the precursor powders of ATLG, such as the ball–mill method,[25] sol–gel auto-combustion process,[26] hydrothermal synthesis method,[27] MSSM,[28] etc. Comparatively, the MSSM as a low-cost, low-temperature, few steps and versatile method can provide a melting-salt environment to form high-quality ATLG powders, further to lay a solid foundation for gaining the highly dense and pure pellets at a lower sintering temperature.[28–30]

In this paper, we successfully synthesize apatite-type $La_{9.33}Ge_6O_{26}$ powders by MSSM through using LiCl and LiCl/NaCl mixture (mass ratio 1:1) as molten salt, and the corresponding synthesis temperature reduces about 350 °C (LiCl), 500 °C (LiCl/NaCl) compared with by using the con-

*Project supported by the Natural Science Foundation of Shandong Province, China (Grant Nos. ZR2016FB16, ZR2015AQ010, and ZR2016AQ08) and the Shandong University of Technology at Zibo and Zibo City Integration Development Project, China (Grant No. 2016ZBXC205).

†Corresponding author. E-mail: sunml@sdut.edu.cn

‡Corresponding author. E-mail: gwei@jlu.edu.cn

© 2018 Chinese Physical Society and IOP Publishing Ltd

ventional SSRM, respectively, which can effectively avoid Ge volatility, agglomeration and crystallinity problems encountered in the conventional preparation process of precursor powders. Furthermore, on the basis of high-quality precursor powders obtained by the MSSM, highly dense and pure ceramic pellets are obtained at a lower temperature of 1100 °C, which exhibit higher conductivities and lower activation energies than those obtained by the conventional SSRM. In addition, the optimal mass ratio between reactant and molten salt, the optimal synthesizing temperature and the associated mechanisms are investigated in detail.

2. Experiment

Original reactant powders of La_2O_3 (purity $\geq$ 99.99%) and GeO_2 (purity $\geq$ 99.99%) were weighed in the stoichiometric composition of $La_{9.33}Ge_6O_{26}$. Before weighing, La_2O_3 powders were precalcined at 1000 °C for 2 h to remove any lanthanum hydroxide or carbonate. The LiCl and LiCl/NaCl mixture (mass ratio 1:1) were taken as eutectic salt and weighed. The mass ratios of reactants to eutectic salt were fixed to be 1:1, 1:2, and 1:3, respectively. Mixtures (reactants and eutectic salt) were further ball-milled, dried, ground, sifted, and calcined at 600 °C–750 °C for 8 h, sequentially. Then the as-synthesized powders were washed repeatedly with de-ionized water and filtered to remove eutectic salt until there was no white precipitate in the filtrate by adding the $AgNO_3$ solution. Finally, $La_{9.33}Ge_6O_{26}$ powders were obtained through drying the products at 110 °C for 12 h. Then the as-synthesized powders were pressed under 100MPa for 30 min and sintered at 1100 °C for 2 h to obtain the dense pellets. In addition, for comparison, the pellets synthesized by conventional SSRM were prepared (the precursor powders were synthesized at 1100 °C for 4 h, and the final pellets were sintered at 1300 °C for 2 h).

Phase identification of samples was carried out by x-ray diffraction (XRD; Shimadu XRD-6000). The data were collected over the 2θ range of 20°–60° in steps of 0.02° by using Cu–Kα radiation. Microstructures of samples were examined by scanning electron microscopy (SEM; JEOL JSM-6700F) and transmission electron microscopy (TEM; JEOL JEM-2200FS). Electrical characterizations of dense pellets were carried out by electrochemical impedance spectroscopy (EIS; Solartron 1260 frequency response analyzer). The Pt electrodes were coated on both surfaces of pellets and sintered at 800 °C for 1 h. The EIS measurements were performed at a 50-°C interval between 300 °C and 850 °C in a frequency range of 0.1 Hz–1 MHz, then the impedance spectrum data were analyzed by Z-View software.

3. Results and discussion

To confirm the optimal mass ratio of reactant and molten salt, the mixtures of reactants and LiCl salt with the mass ratios of 1:1, 1:2, and 1:3 are calcined at 650 °C, 700 °C, and 750 °C according to the melting temperature of molten salt (see Fig. 1), respectively. The corresponding XRD patterns are shown in Fig. 2. It can be concluded that the apatite structure cannot be acquired when the mass ratios are 1:1 and 1:3 at different temperatures, which implies that these two mass ratios are unsuitable for synthesizing apatite-type $La_{9.33}Ge_6O_{26}$ powders. It is mainly because the original reactant powders (La_2O_3 and GeO_2) cannot completely dissolve in the melting-salt environment when the mass ratio is of 1:1, but too much melting-salt environment will inhibit the precipitation of $La_{9.33}Ge_6O_{26}$ powders as the mass ratio is 1:3. In contrast, the apatite structure is obviously observed as the middle mass ratio of 1:2, and a pure apatite phase without any impurity is obtained at a calcining temperature of 750 °C, which indicates that the middle mass ratio of 1:2 is optimal, because this proper melting-salt environment can simultaneously ensure the good dissolution of original reactant powders and the good precipitation of $La_{9.33}Ge_6O_{26}$ powders. Comparing with the SSRM, the calcining temperature is much lower than 350 °C, which can effectively inhibit Ge loss and reduce energy consumption when preparing the precursor powders. However, there is a problem as LiCl salt is difficult to remove. In order to overcome this drawback, the proper NaCl is incorporated into LiCl as eutectic salt. Experimental results indicate that the LiCl/NaCl mixed salts with the mass ratio of 1:1 can effectively solve the above problem. More excitingly, the pure apatite-type $La_{9.33}Ge_6O_{26}$ powders are successfully synthesized at a lower temperature of 600 °C (see Fig. 3) due to the lower melting temperature of mixed salts (see the inset of Fig. 1), which is more than 550 °C lower than that of the molten-salt synthesis method.

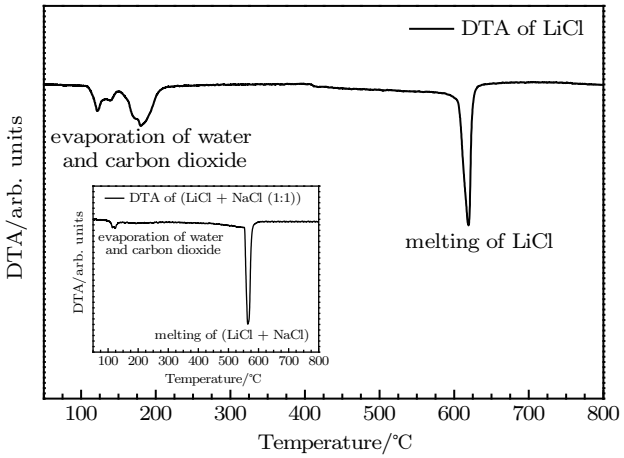


Fig. 1. DTA curve of LiCl salt among 50 °C–800 °C in air, and the inset is DTA curve of LiCl/NaCl mixed salts (mass ratio 1:1) among 50 °C–800 °C in air.

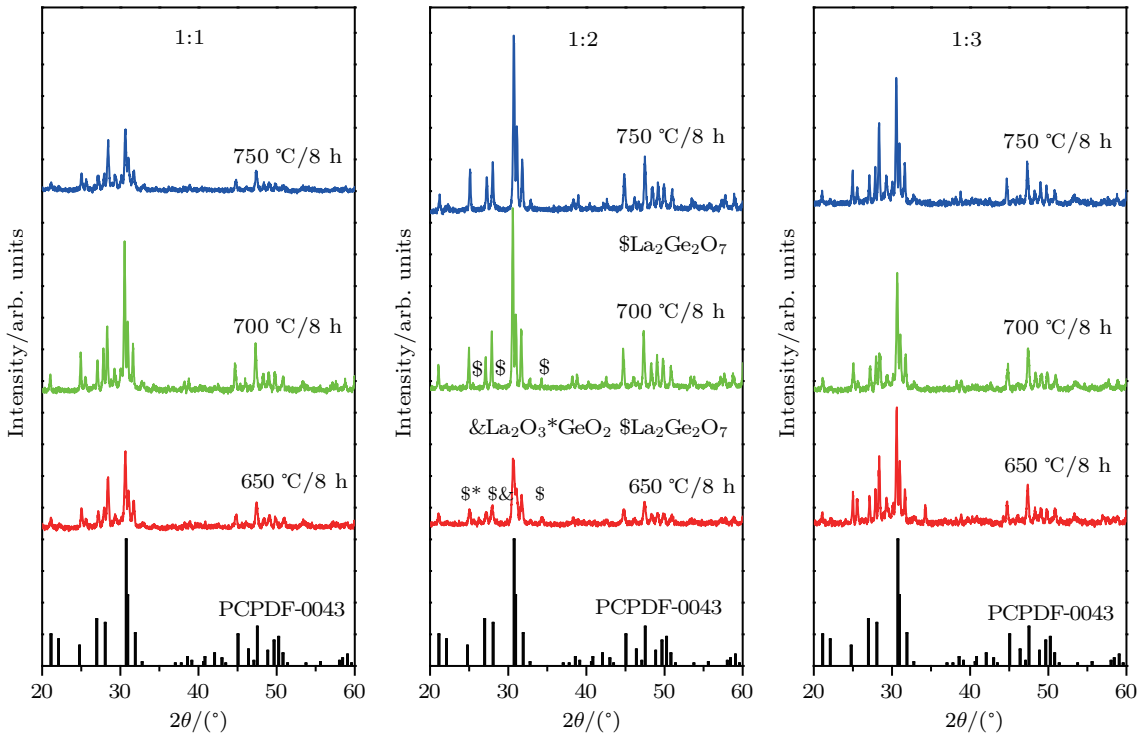


Fig. 2. (color online) XRD patterns of the powders synthesized by LiCl MSSM with different mass ratio of reactants and LiCl salt (1:1, 1:2, and 1:3) at 650 °C, 700 °C, and 750 °C for 8 h, respectively.

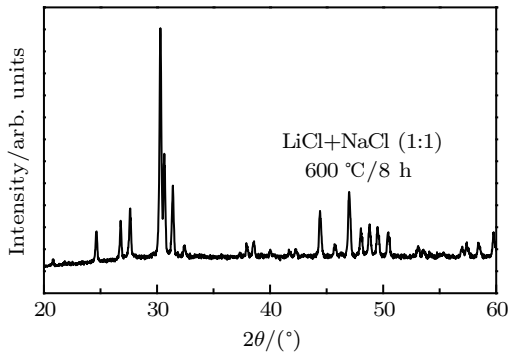


Fig. 3. XRD pattern of the powders synthesized by LiCl/NaCl MSSM at 600 °C for 8 h.

The microstructure of $La_{9.33}Ge_6O_{26}$ powders synthesized by MSSM are displayed in Fig. 4. As shown in the figure, the as-synthesized powders are nano-sized, homogeneous and less agglomerated particles, which should be ascribed to the effect of the melting-salt environment. The melting-salt environment can promote the dispersion of reactants to make them realize an atomic/molecule-scale reaction, which, meanwhile, can exist around the growing particles to effectively inhibit the agglomeration and control the particle sizes. Compared with the SSRM, the MSSM can effectively solve the main problems such as Ge volatility, agglomeration and crystallinity encountered in the preparation of precursor powders, and the high-quality precursor powders are obtained, which will be more beneficial for gaining the dense and pure pellets. In addition, it can be seen that the $La_{9.33}Ge_6O_{26}$powders synthesized in LiCl/NaCl mixed melting-salt environment are more homogeneous than that synthesized in the LiCl individual melting-salt environment, and the corresponding particles have an average size of around 200 nm.

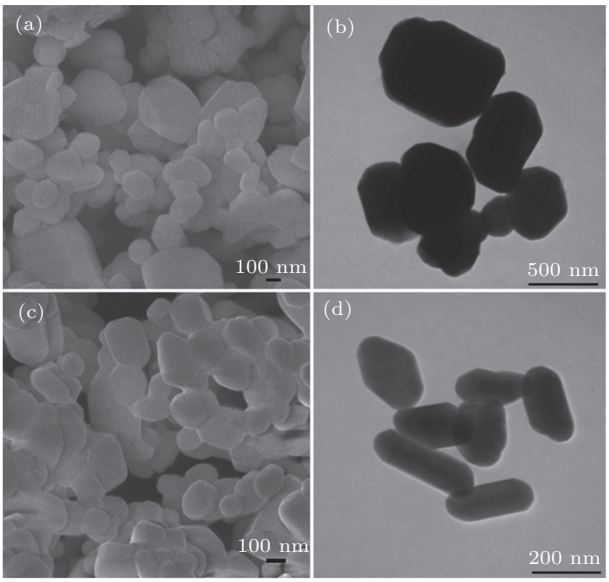


Fig. 4. SEM (a) and TEM (b) images of $La_{9.33}Ge_6O_{26}$ powders obtained by LiCl MSSM at 750 °C for 8 h; and SEM (c) and TEM (d) images of $La_{9.33}Ge_6O_{26}$ powders obtained by LiCl/NaCl MSSM at 600 °C for 8 h.

On the basis of high-quality precursor powders, the proper pellets are sintered at 1100 °C (which is lower than the melting point of GeO_2) for 2 h. The low sintering temperature and short sintering time can effectively avoid the high-temperature Ge loss problem encountered in conventional SSRM, which can be confirmed by the XRD pattern

of pellets in Fig. 5. As shown in the figure, the proper pellet has a pure hexagonal apatite-type structure with no impurity (La_2GeO_5). Moreover, the relative density of pellets reaches a high level of ~95% measured by the Archimedean method, which can be illustrated by the SEM images of pellets (Fig. 6). In addition, the pellets obtained by the more homogeneous precursor powders that are synthesized in LiCl/NaCl melting-salt environment have fewer grain boundaries, which should be more useful for oxide-ion conduction.

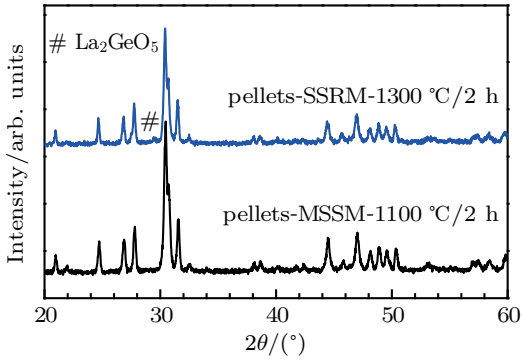


Fig. 5. (color online) XRD patterns of $La_{9.33}Ge_6O_{26}$ pellets obtained by MSSM at 1100 °C for 2 h and the compared pellets sintered by SSRM at 1300 °C for 2 h.

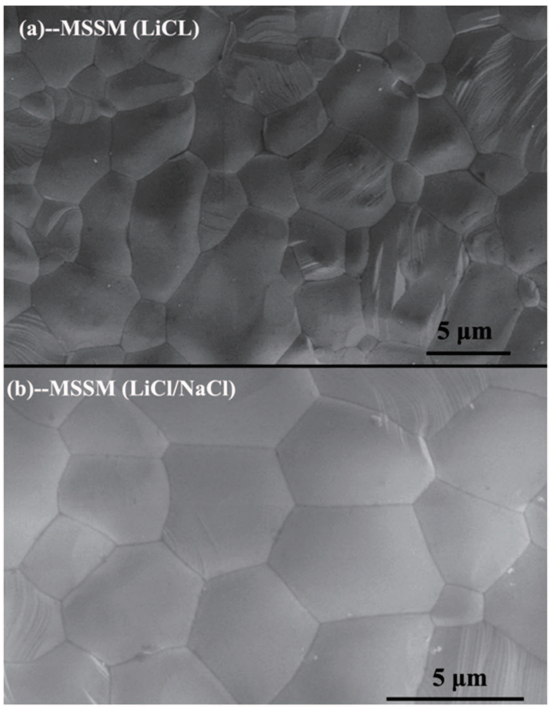


Fig. 6. SEM images of the pellets prepared by the powders obtained by LiCl (a) and LiCl/NaCl, (b) MSSM at 1100 °C for 2 h.

The electrochemical impedance of ceramic pellets are measured in air from 300 °C to 850 °C in steps of 50 °C, and the complex impedance plots measured at 300 °C, 550 °C, and 700 °C are displayed in Fig. 7. In order to distinguish the contributions of bulk, grain boundary and electrode, the corresponding contributions are analyzed with the Z-View software by modeling the impedance spectrum with the equivalent circuit including four serial R_i and $(CPE)_i$ parallels (i refers to "bulk" for bulk, "gb" denotes the grain boundary and "elec" the electrode). As shown, the impedance spectrum measured at 300 °C exhibits two independent semicircular arcs and a straight line from high frequency to low frequency, which corresponds to the conduction across the bulk (R_{bulk}), the conduction across grain boundary (R_{gb}) and the impedance response corresponding to electrode (R_{elec}), respectively. With the increasing of temperature, the arc corresponds to the grain contributions gradually disappearing, and the arc or spike corresponds to the grain boundary and electrode shifted to higher frequencies as shown in the impedance spectrum measured at 500 °C. When the temperature is beyond 700 °C, the arcs corresponding to the grain and grain boundary contributions disappear, and only an arc ascribed to the contribution of the electrode is observed, which indicates that the oxide-ion could diffuse through the entire thickness of bulk and grain boundary. Furthermore, the dense pellets sintered by more homogeneous precursor powders that are synthesized in LiCl/NaCl mixed melting-salt environment exhibit a better electrical property, which should be attributed to the higher density and fewer grain boundaries.

The corresponding conductivity is converted by the resistance R using Eq. (1), and the activation energy is calculated by the Arrhenius equation (2):

$$\sigma = l/(R \cdot S), \tag{1}$$

$$\sigma = \sigma_0 * \exp[-E_a/(k \cdot T)]/T, \tag{2}$$

where l, S, σ, σ_0, E_a and T are, respectively, the sample thickness, the electrode area of the sample surface, the conductivity, the pre-exponential factor, the activation energy, the Boltzmann constant and the absolute temperature.

The conductivities of pellets prepared by MSSM and SSRM at different temperatures are plotted in Arrhenius plots (Fig. 8). As shown, the pellets obtained by MSSM exhibit evidently higher conductivities than by SSRM. The $La_{9.33}Ge_6O_{26}$ pellets prepared by the MSSM exhibits excellent conductivities with values of 2.3×10^{-2} S·cm^{-1} (LiCl) and 4.9×10^{-2} S·cm^{-1} (LiCl/NaCl) at 850 °C, respectively, which are higher than those of the pellets with the same compositions reported in Refs. [24]–[26], [31], and [32]. Furthermore, the corresponding activation energy is calculated by the Arrhenius equation. The activation energies ($E_{a(LiCl)}$ = 1.02 eV, $E_{a(LiCl/NaCl)} = 0.99$ eV) of pellets prepared by MSSM are lower than those ($E_{a(SSRM)} = 1.09$ eV) of pellets prepared by SSRM, which should be ascribed to the high density, no impurity and fewer grain boundaries. In addition, consistent with the fewer grain boundaries, the dense pellets obtained by LiCl/NaCl MSSM exhibit a higher conductivity and a lower activation energy than those obtained by LiCl MSSM, which is consistent with the case of fewer grain boundaries.

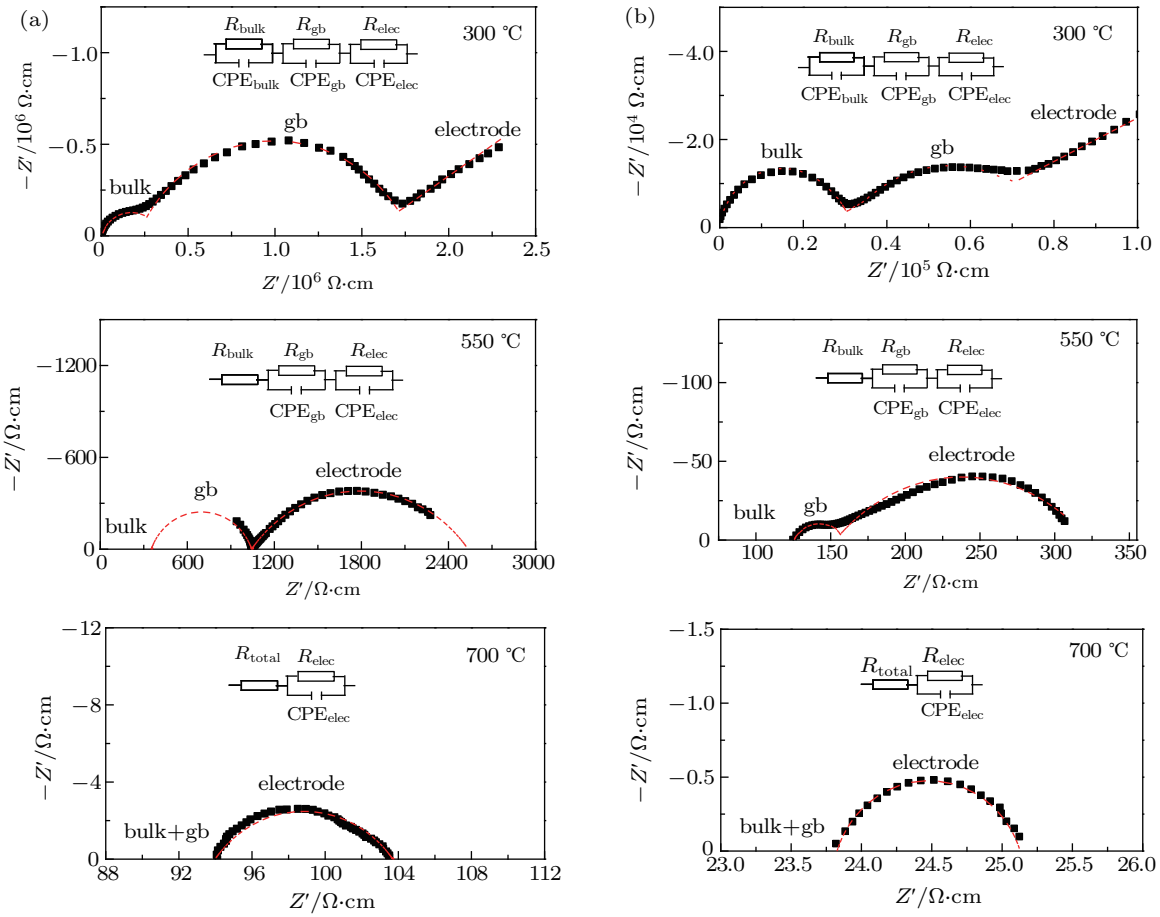


Fig. 7. (color online) Electrochemical impedance spectra of $La_{9.33}Ge_6O_{26}$ pellets sintered by the powders obtained by LiCl (a) and LiCl/NaCl (b) MSSM measured at 300 °C, 550 °C, and 700 °C, and the corresponding schematic equivalent circuits.

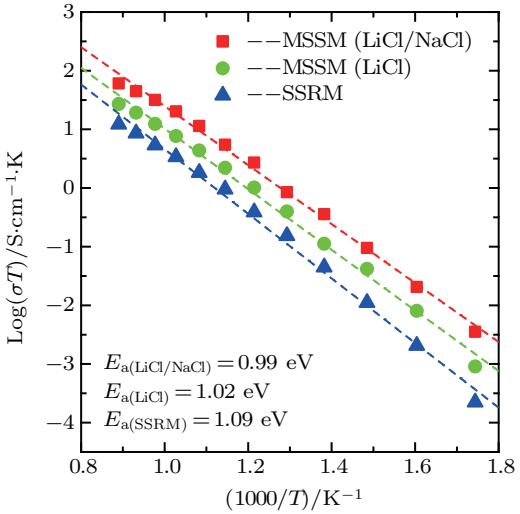


Fig. 8. (color online) Arrhenius plots for the conductivity of $La_{9.33}Ge_6O_{26}$ pellets sintered by MSSM at 1100 °C and the compared pellets sintered by SSRM at 1300 °C.

4. Conclusions

High-quality $La_{9.33}Ge_6O_{26}$ powders with apatite structure are successfully synthesized via a facile MSSM by using LiCl, LiCl/NaCl mixture (mass ratio 1:1) as molten salt, respectively. The optimal mass ratio of reactant and molten salt is 1:2, and LiCl/NaCl mixed molten-salt is more beneficial for synthesizing high-quality $La_{9.33}Ge_6O_{26}$ powders. Compared with the SSRM, the MSSM can evidently reduce the synthesis temperature to aviod Ge loss and obtain homogeneous, non-agglomerated and well crystallized powders. Furthermore, the dense and pure ceramic pellets of $La_{9.33}Ge_6O_{26}$ are obtained at 1100 °C for 2 h, which exhibit higher conductivity and lower activation energy than those obtained by the SSRM, due to their high density, no impurity and fewer grain boundaries. Additionally, the dense pellets obtained by LiCl/NaCl MSSM exhibit the best conductivity and lowest activation energy.

References

[1] Matsunaga K, Imaizumi K, Nakamura A and Toyoura K 2017 *J. Phys. Chem. C* **121** 20621
[2] Vitorino N, Oliveira F A C, Marcelo T, Abrantes J C C and Trindade B 2017 *Ceram. Int.* **43** 3847
[3] Dai L, Han W, Li Y H and Wang L 2016 *Int. J. Hydrogen Energy* **26** 11340
[4] Dong X F, Hua G X, Dong D, Zhu W L and Wang H J 2016 *J. Power Sources* **306** 630
[5] Cao X G, Jiang S P and Li Y Y 2015 *J. Power Sources* **293** 806
[6] Imaizumi K, Toyoura K, Nakamura A and Matsunaga K 2014 *Solid State Ionics* **262** 512
[7] Yin G C, Yin H, Wang X, Sun M L, Zhong L H, Cong R D, Zhu H Y, Gao W and Cui Q L 2014 *J. Alloys Compd.* **611** 24

[8] Yin G C, Yin H, Zhu H Y, Wu X X, Zhong L H, Sun M L, Cong R D, Zhang J, Gao W and Cui Q L 2014 *J. Alloys Compd.* **586** 279
[9] Wang S F, Hsu Y F, Lin W J and Kobayashi K 2013 *Solid State Ionics* **247** 48
[10] Yin G C, Yin H, Zhong L H, Sun M L, Zhang J K, Xie X J, Cong R D, Wang X, Gao W and Cui Q L 2014 *Chin. Phys. B* **23** 048202
[11] Santos M, Alves C, Oliveira F A C, Marcelo T, Mascarenhas J, Cavaleiro A and Trindade B 2013 *J. Power Sources* **231** 146
[12] Liu W, Yamaguchi S, Tsuchiya T, Miyoshi S, Kobayashi K and Pan W 2013 *J. Power Sources* **235** 62
[13] Fukuda K, Asaka T, Okino M, Berghout A, Béchade E, Masson O, Julien I and Thomas P 2012 *Solid State Ionics* **217** 40
[14] Orera A, Baikie T, Panchmatia P, White T J, Hanna J, Smith M E, Islam M S, Kendrick E and Slater P R 2011 *Fuel Cells* **1** 10
[15] Yamagata C, Elias D R, Paiva M R S, Misso A M and Mello Castanho S R H 2013 *Mater. Res. Bull.* **48** 2227
[16] Desclaux P, Nurnberger S, Rzepka M and Stimming U 2011 *Int. J. Hydrogen Energy* **36** 10278
[17] Courtin E, Boy P, Piquero T, Vulliet J, Poirot N and Laberty-Robert C 2012 *J. Power Sources* **206** 77
[18] Ishihara T, Matsuda H and Takita Y 1994 *J. Am. Chem. Soc.* **116** 3801
[19] Li B, Liu W and Pan W 2010 *J. Power Sources* **195** 2196
[20] Béchade E, Masson O, Iwata T, Julien I, Fukuda K, Thomas P and Champion E 2009 *Chem. Mater.* **21** 2508
[21] Abram E J, Kirk C A, Sinclair D C and West A R 2005 *Solid State Ionics* **176** 1941
[22] Tolchard J R, Sansom J E H, Sansom P R and Islam M S 2004 *J. Solid State Electrochem.* **8** 668
[23] Kendrick E, Headspith D, Orera A, Apperley D C, Smith R I, Francesconi M G and Slater P R 2009 *J. Mater. Chem.* **19** 749
[24] Sansom J E H, Hildebrandt L and Slater P R 2002 *Ionics* **8** 155
[25] Tian C G, Liu J L, Guo C J, Cai J, Cai T X and Zeng Y W 2008 *J. Alloys Compd.* **60** 646
[26] Rodriguez-Reyna E, Fuentes A F, Maczka M, Hanza J, Boulahya K and Amador U 2006 *Solid State Sci.* **8** 168
[27] Li H, Baikie T, Pramana S S, Shin J F, Keenan P J, Slater P R, Brink F, Hester J and White T J 2014 *Inorg. Chem.* **53** 4803
[28] Yin G C, Yin H, Sun M L, Zhong L H, Zhang J K, Cong R D, Gao W and Cui Q L 2014 *RSC Adv.* **4** 15968
[29] Huang Z X, Li B Y and Liu J 2010 *Phys. Status Solidi* **207** 2247
[30] Li B Y, Liu J, Hu Y X and Huang Z X 2011 *J. Alloys Compd.* **509** 3172
[31] Sansom J E H and Slater P R 2004 *Solid State Ionics* **167** 23
[32] Sansom J E H, Najib A and Slater P R 2004 *Solid State Ionics* **175** 353